The high voltage system the novel MPGD-based photon detectors of COMPASS RICH-1 and its development towards a scalable HVPSS for MPGDs

Stefano Levorato on behalf of the COMPASS RICH-1 group

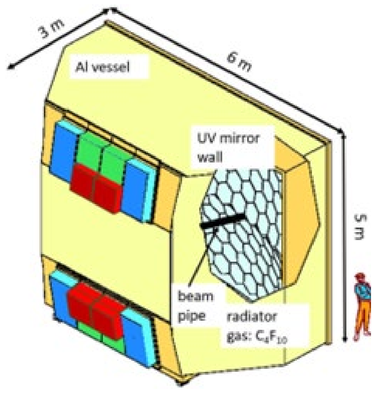

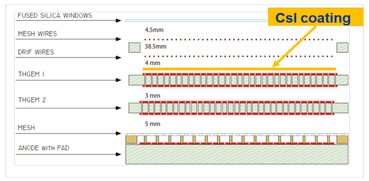

Figure 1: (Left) the COMPASS RICH-1, and the sketch of the hybrid single photon detector: two staggered THGEM layers are coupled to a bulk MicroMegas. The drift wire and protection plane are visible. Not to scale.

During the 2015-16 winter shut-down of the COMPASS experiment, approximately 1.4 m^2 of the active area of the RICH-1 Photon Detectors (PD) was upgraded by novel detectors based on Micro Pattern Gaseous Detector technologies.

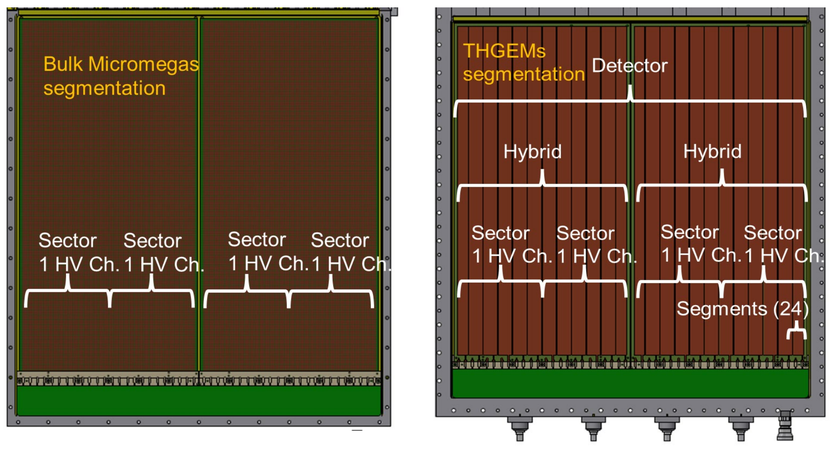

Figure. 2. Detector electrical segmentation scheme and nomenclature. Left MicroMegas segmentation. Right THGEM segmentation.

The architecture of the novel detectors, illustrated in Fig. 1,combines in a hybrid MPGD arrangement two layers of Thick GEMs (THGEM) to a MicroMegas (MM). The top surface of the first THGEM 600 × 300 mm^2 is coated with a CsI film which acts as a reflective photo-cathode. The THGEMS are 0.4 mm thick, hole diameter and pitch are 0.4 mm and 0.8 mm respectively. Both THGEM layers are electrically divided in 12 segments (Fig. 2). The MM uses a pad segmented anode with a pad size of 7.5 × 7.5 mm^2 and 8 mm pitch (Fig .3). Each hybrid detector is made by two 600 × 300 mm^2 modules placed side by side to form a single unit. Each MM module is electrically segmented into two sectors and biased according to the scheme in Fig 4.

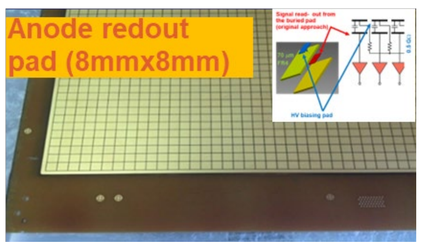

Figure 3: HV is applied to the anode pads by individual 470 MΩ resistors, while the signals are collected from a second set of pads, embedded in the anode PCB, where the signal is transferred by capacitive coupling. The large-value resistance decouples each pads from the neighboring ones in case of occasional discharges limiting the voltage (gain) drop to 2V 28 (4%)

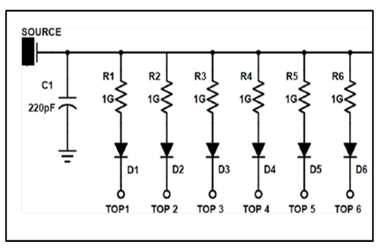

Figure 4: Scheme of the voltage distribution to six THGEM segments of the top (bottom) face. Each sector is powered via a single HV channel through a distribution scheme employing a 1 GΩ resistors and fast 20ETS12S1 diodes to prevent the current flow from a segment to the others in case of a discharge.

The detectors are operated with the gas mixture Ar: CH4 = 50: 50, selected for optimal extraction of the photo-electrons from the converting CsI film to the gaseous atmosphere. The typical voltages applied to the detector electrodes are 1270 V across THGEM1, 1250 V across THGEM2, and 620 V to bias the MM. The drift field above the first THGEM is 500 V/cm, the transfer field between the two THGEMs is 1000 V/cm and the field between the second THGEM and the MM micromesh is 1000 V/cm

$$V(P,T) = V_0(1+0.5(P/P_0 \cdot T_0/T - 1))$$

Equation 1: V is the voltage, P is the absolute pressure in mbar, T is the temperature in degrees Kelvin and V_0, T_0 and P_0 refer to reference conditions.

HV channel setting within a detector is highly correlated, making the correct manual operation a complex and risky task. Therefore, a custom-made control system has been realized; The reference HV values are accompanied by individual *OwnScale* of each channel to make fine-tuning for gain uniformity easier. An auto decrease HV algorithm is implemented to protect the detectors in case of a too high current spark rate. The voltage and current monitored by the power supply are logged at 1 Hz rate. The Block diagram is illustrated in Fig. 5. The voltages are continuously corrected on the base of the measured environmental parameters, namely temperature and pressure, in order to preserve the detector gain stability according to the equation 1.

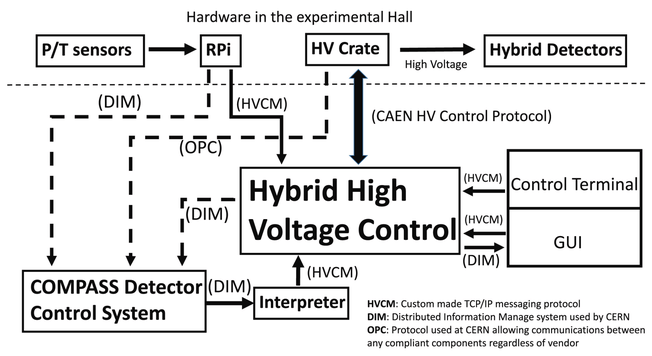

Figure. 5. Block diagram of the hybrid high voltage control system, showing the components and their communication channels.

Commercial power supply units by CAEN are used. THGEM electrodes as well as the protection wires, the drift wires and the lateral auxiliary electrodes are powered by A1561HDN 12-channel modules. MM pads are supplied by A7030DP 12-channel modules for which a variation of the off-set of the current monitoring has been observed during operation. They are hosted in the SY4527 mainframe, for fast access to the monitoring/control options via a Gigabit Ethernet interface. In total, the supply system for the four detector sets includes nearly **140 channels**.

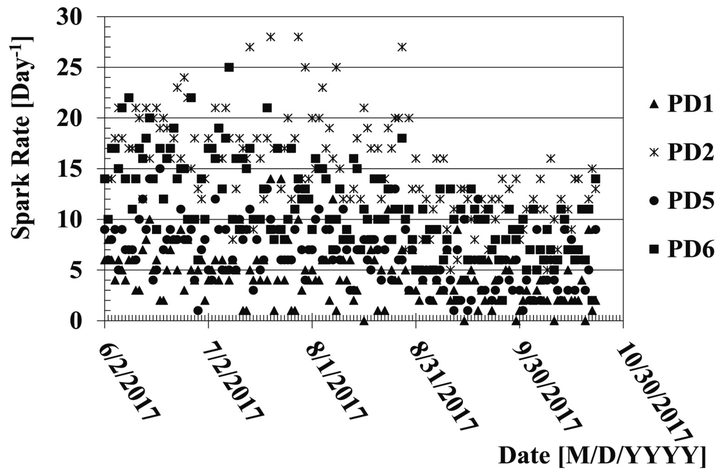

Figure. 6. Spark rate counting (in unit of per day) for all four hybrid detectors during physics data taking of year 2017.

In the hybrid MPGDs installed in RICH-1, discharges result in short current spikes, thanks to the resistive protection applied in the supply schemes of both THGEMs and MMs. The power supply parameters reading at 1 Hz makes it possible to know the duration of the spikes and the corresponding restoration time. MM spikes have a duration of 1–2 s, while THGEM spikes last 10 s. The order of magnitude of these recovery times corresponds to the time required for loading the equivalent RC systems. These short duration combined with the very low spike rate of the order of 1/h (Fig. 6) per detector and the detector segmentation, which limits the area affected by a spark, makes the dead-time caused by detector sparks totally negligible.

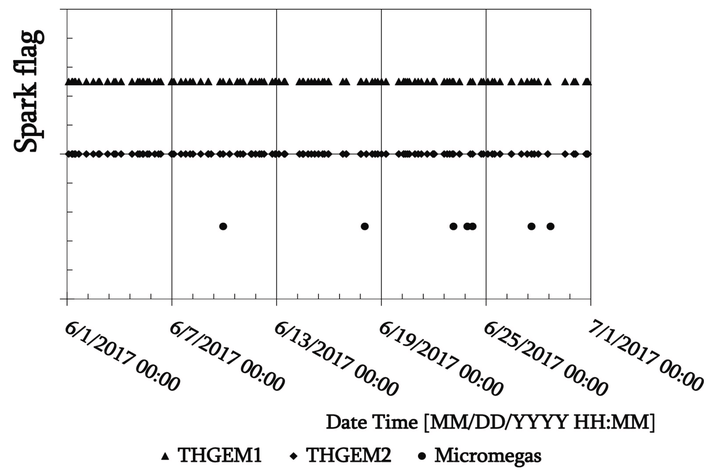

Figure 7: Correlation of the current sparks among three multiplication stages. A marker in the top (middle) row illustrates a current spark in the THGEM1 (THGEM2). A marker in the bottom row illustrates a current spark in the Micromegas. All the sparks are aligned as a function of time. Data show that sparks in the two THGEMs layers are 100% correlated, while a spark in MM is accompanied by a spark in THGEMs in 70% of the cases.

The sparks can be correlated among the different multiplication stages of a detector sector (Fig. 7). Sparks in the two THGEM layers of a sector are 100% correlated. This is expected taking into account that a spark results in a temporary short between the two THGEM electrodes, with a drastic local variation of the electric field that affects also the other THGEM layer. The spark rate in MM is low compared to THGEMs, proving that the implemented resistive MM scheme results in an intrinsically robust multiplication stage. MM sparks are accompanied by sparks in THGEMs in 70% of the cases as illustrated in Fig 7.

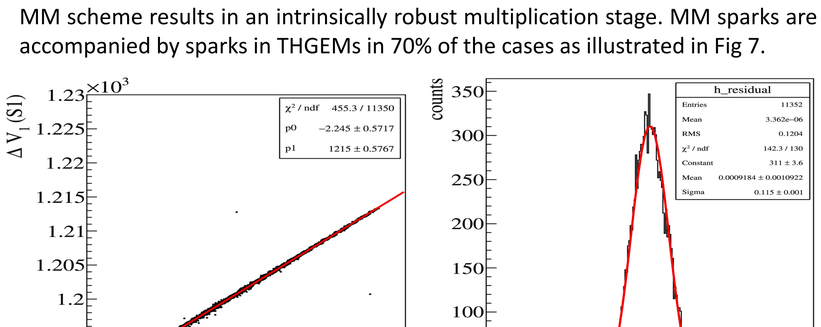

Figure. 8. (Left) (unit V) of sector 1 of the first THGEM in one particular detector as a function of correction factor. The red line is a linear fit to the data points. (right) The residual of the data points and the linear fit in the left plot.

The correct application of the voltage correction is demonstrated by the example in Fig. 8. In Fig. 8, left, where the voltage variation is drawn versus the voltage correction factor for the first THGEM of one sector of one photon detector. The points of the graph are very well aligned around the fitted straight line. This indicates that the linear correction due to temperature and pressure fluctuations is implemented correctly. The residual between the data points and the linear fit is shown Fig. 8 right. The width of the Gaussian fit indicates that the correction resolution is around 0.1 V, matching the voltage resolution setting of the power supply.

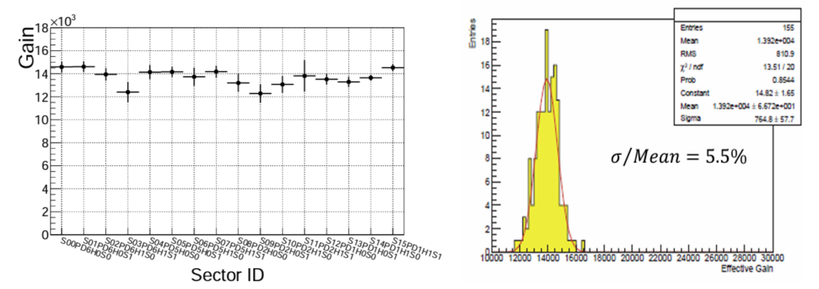

Figure. 9. (Left) Effective gain as function of the different detector sectors. Right: the effective gain distribution during several days of detector operation.

The remarkable gain uniformity obtained with the fine-tuning options described by correcting the voltage for P and T variation is shown in Fig. 9, where the gain is estimated from the single photon exponential spectra. On the left the effective gain is plot as function of the different sectors of the Hybrid Photon detector. On the right the effective gain distribution extracted from the data during several days of detector operation for one sector only. It shows a standard deviation of approximately 5.5%, an excellent result despite the possible limitations related to the temperature non uniformity of the gas in the detector and the linear approximation of the equation 1.

The development of a High Voltage Power Supply System (HVPSS) suited for the MPGD technologies originates from the experience gained in upgrading COMPASS RICH-1 with MPGD-based single photon detectors. The system has been designed and built to match all the requirements for the complete monitoring and the accurate handling of MPGDs, also those that cannot be satisfied using commercial power supply systems: time stamp resolution for current monitoring in the order of 10 ns or better; high voltage resolution monitoring better than 0.5 Volt on several kV scale, precise current monitoring at the level of 10 pA, on board logic for decisional operation on predefined monitored parameters/conditions well as warning on interesting events to the user.

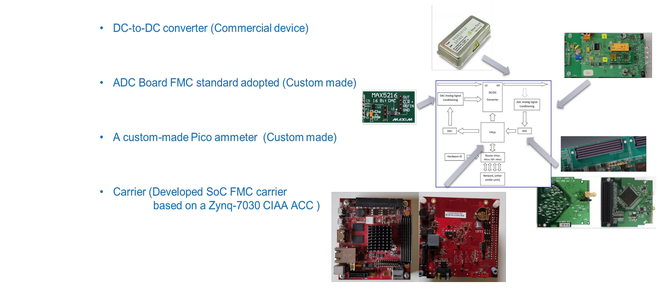

Figure. 10. HVPSS building elements. The block scheme, in the center, illustrates the data flow between the components.

The HVPSS (Fig 10) is composed of a commercial DC / DC converter based on the ISEG5 108 BPn4010512 module. The voltage control of the DC-to-DC converter is obtained via a 16-bit DAC MAX52166 galvanically isolated through a high-performance quad-channel digital isolator ISO7841DWW7. A custom made picoammeter board is built around a AD549LHZ8 operational amplifier operated in trans-conductance mode. A dedicated data acquisition board for high-speed Analog to Digital Conversion (ADC) has been built employing the low power 8-bit high speed 500 MSPS ADC08500 device. The current resolution of the picoammeter coupled with this ADC spans from 3.9 pA at 0.95 MHz to 65.2 pA at 250 MHz, within a full range of 60nA.
The CIAA-ACC, an open hardware industrial System-on-Chip SoC carrier has been selected for data acquisition and system operation handling. It houses a Xilinx Zynq 7030 FPGA and microprocessor SoC in a high pin count. Logic cores designed and implemented in the FPGA subsystem handle the data acquisition and time-deterministic tasks such as raw data sampling, timestamping, signal analysis and diagnostics, hardware peripheral control, and the communication between the FPGA and microprocessor.

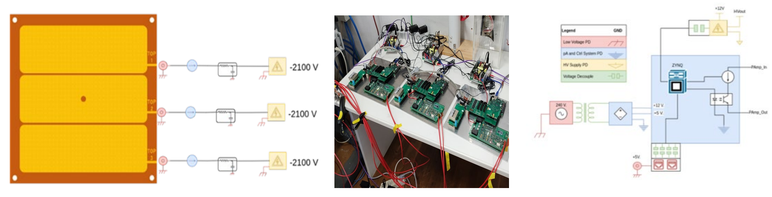

Figure. 11. (Left) Connection scheme of the 3 HVPSSs to the different THGEM sectors. Center, image of the setup. The HV and grounding isolation scheme.

A three channel HVPSS system has been operated connected to independent segments of the first THGEM layer of a hybrid photon detector (Fig 11). Multichannel time synchronization has been obtained via Precision Time Protocol (PTP).

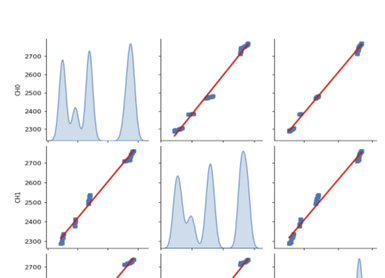

Figure 12. Pairwise scatter plot matrix of discharge times of three neighboring HV channels

The THGEMs electrodes have been biased 10% more than the typical operating voltage resulting in a large rate of discharges between the top and bottom layer of the THGEM. A comparison of the current spikes as a function of the detection time taken during several minutes is plotted for the three different channels in Fig. 12. The red line correspond to fully correlated events, the diagonal the density estimation plot of the time distribution of the electrical discharges on each channel.

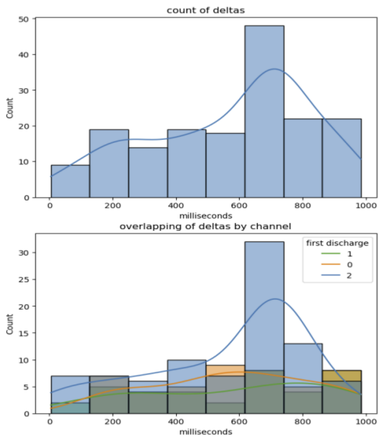

Figure 13: Histogram of time difference (deltas) after primal discharge in a one second window and the contribution of each channel into the discharge

By choosing an electrical discharge as primal and measuring the elapsed time for the next one in a one-second window, a peak value of around 600 to 700 milliseconds can be seen in Fig. 13. As shown in the plot, one of the three channels presents a higher contribution to these events.
Systematic tests are ongoing trying to improve the 20 ns maximum time uncertainty measured between the different HVPSS system synchronization systems via the PTP protocol.